ciety Handbooks (Bios Scientific, Oxford, 1994), vol. 27.

23. Total cell numbers (cells per milliliter) and standard errors (in percent) for Fig. 1. Standard errors are only listed for organisms detected. **A drift: Flow:** 1.8×10^6 cells, *L. ferrooxidans* (*Lf*) ±15%, Bacteria (Bac.) ±9%, Eukarya (Euk.) ±2%, Archaea (Arch.) ±2%; **Pool:** 6.3×10^4 cells, Bac. ±11%, Euk. ±3%; **Spill.:** 1.4×10^6 cells, *Lf* ±12%, Arch. ±2%, Euk. ±5%, Bac. ±8%; **Slime1:** 2.4×10^9 cells, *Lf* ±8%, Bac. ±12%, Euk. ±7%; **Slime2:** 1.3×10^9 cells, *Lf* ±6%, Bac. ±9%, Euk. ±7%; **Sed.:** 2.2×10^7 cells, *Lf* ±4%, Bac. ±6%, Euk. ±2%. **C drift: Flow:** 4.8×10^6 cells, *Lf* ±3%, Bac. ±7%; **Spill.:** 5.2×10^3 cells, *Lf* ±4%, Bac. ±8%, Arch. ±2%; **Slime:** 4.3×10^8 cells, *Lf* ±12%, Bac. ±14%, Euk. ±6%; **Sed.:** 7.3×10^5 cells, Bac. ±11%, *Lf* ±2%. **Tunnel: Matte:** 2.4×10^5 cells, Bac. ±9%; **Slime1:** 5.7×10^9 cells, *Lf* ±5%, *T. ferrooxidans* (*Tf*) ±9%, Bac ±4%; **Slime2:** 3.8×10^9 cells, *Lf* ±3%, *Tf* ±8%, Bac. ±6%; **Slime3:** 1.1×10^9 cells, *Lf* ±3%, *Tf* ±9%, Bac. ±8%; **Slime4:** 9.1×10^9 cells, *Lf* ±6%, *Tf* ±4%, Bac. ±6%; **Slime5:** 4.7×10^9 cells, *Lf* ±5%, *Tf* ±9%, Bac. ±5%.

24. We thank T. Rodgers, J. Ireland, C. Alpers, S. Bintrim, and D. K. Nordstrom for their input to this study; S. Bintrim, R. Spear, and A. Tsang for providing cultures; and Iron Mountain Mine Inc. and Stauffer Management Co. for making this work possible. Funding was provided by NSF grant CHE-9521731, EPA grant CR822902-01-0, and a grant from the McKnight Foundation.

13 November 1997; accepted 26 January 1998

Materials with Negative Compressibilities in One or More Dimensions

Ray H. Baughman,* Sven Stafström, Changxing Cui,
Socrates O. Dantas

Rare crystal phases that expand in one or more dimensions when hydrostatically compressed are identified and shown to have negative Poisson's ratios. Some of these crystals (i) decrease volume and expand in two dimensions when stretched in a particular direction and (ii) increase surface area when hydrostatically compressed. Possible mechanisms for achieving such negative linear and area compressibilities are described for single crystals and composites, and sensor applications are proposed. Materials with these properties may be used to fabricate porous solids that either expand in all directions when hydrostatically compressed with a penetrating fluid or behave as if they are incompressible.

Most materials contract in all directions when hydrostatic pressure (P) is applied—that is, the volume compressibility ($-dV/VdP$), area compressibilities ($-dA/AdP$), and linear compressibilities ($-dL/LdP$) are all positive. Materials are thermodynamically forbidden to have negative volume compressibilities. A negative area compressibility was initially reported for a trigonal phase of arsenic (*1*), but this result disagrees with later measurements (*2*). However, there are rare reports of crystals having negative linear compressibilities: lanthanum niobate (*3*), cesium dihydrogen phosphate (*4*), an orthorhombic high-pressure paratellurite (TeO_2) phase (*5*), and the isomorphous trigonal Se and Te phases (*6, 7*).

A solid increases density when stretched along an axis of negative linear compressibility, so it is equivalent either to say that a solid has the property of being stretch densified or that it has a negative linear compressibility. If we denote the elastic compliance coefficients for arbitrary orthogonal axes as S_{ij}', then $S_{11}' + S_{12}' + S_{13}'$ is the linear compressibility in the x'-axis direction and $S_{11}' + S_{21}' + S_{31}'$ is the corresponding coefficient for the fractional volume change produced by a uniaxial stress in the x'-axis direction. The elastic constant matrix is symmetric (*8*), so that $S_{ij}' = S_{ji}'$, and therefore these coefficients for pressure-induced linear dimension change and stretch-induced volume change are equal.

By using well-known equations (*8*) for linear compressibility as a function of elastic compliances (S_{ij}), it is easily seen that both the minimum and maximum of linear compressibility occur in crystal-axis directions for orthorhombic or higher symmetry phases. Whereas the existence of only positive linear compressibilities constrains the magnitude of any individual linear compressibility to be less than the bulk compressibility, this constraint disappears if any linear compressibility is negative. We will use experimental data to identify phases where a positive linear compressibility exceeds the bulk compressibility, so the area compressibility (which is the difference between the bulk and the linear compressibility) is negative for a plane perpendicular to the direction of this positive compressibility. This implies that there are negative linear compressibilities for two perpendicular directions within this plane. By choosing a plane with a negative area compressibility as the predominant crystal face, a crystal can be obtained whose total surface area increases with increasing hydrostatic pressure.

We searched for evidence of stretch-densified phases, using the elastic constant tensors that have been experimentally determined for about 500 noncubic crystal phases (*7*). Only about 13 of the 500 investigated compositions are stretch densified (Table 1). Other than the tetragonal mercurous halide phases and the trigonal chalcogen phases, there are no convincing examples of stretch densification in the elastic-constant tabulations for about 270 different hexagonal, tetragonal, and trigonal phases (*7*). Out of 145 tabulated orthorhombic phases (*7*), only cadmium formate, calcium formate, cesium biphthalate, *m*-dihydroxybenzene, 3-methyl 4-nitropyridine 1-oxide, and tris-sarcosine calcium chloride provide data that are clearly consistent with stretch densification. No stretch-densified triclinic phases were identified, and 70 investigated monoclinic phases provide three likely examples of stretch-densified phases: ethylene diamine tartrate, cesium dihydrogen phosphate, and lanthanum niobate.

Each of the stretch-densified crystal phases in Table 1 provides both positive and negative values for the Poisson's ratio, which is the ratio of a lateral contraction to a longitudinal elongation produced by a tensile stress. In fact, Se, the two tetragonal phases, and all three monoclinic phases both increase density and expand in one lateral direction when stretched along a particular direction. However, few crystals with a negative Poisson's ratio have a negative linear compressibility. Equally interesting, a negative area compressibility results for the reported elastic constant tensor (*3, 7*) for monoclinic cesium dihydrogen phosphate and lanthanum niobate, and possibly for orthorhombic cadmium formate.

To enable the design of materials with negative linear compressibilites, we identified several basic structural types that lead to this property. Mechanical and molecular models for hinged structures can be constructed (Fig. 1) in which stretch densification results from a wine-rack–like deformation mode, like those for proposed polydiacetylene carbon phases (*9*). Molecular mechanics calculations suggest (Fig. 1C) (*10*) that ferroelasticity (and associated shape memory behavior) should occur in combination with negative linear compressibilities for particular hinged structures. Both properties are observed for Hg_2Br_2, Hg_2I_2, lanthanum niobate, and tris-sarcosine calcium chloride (*7*). Munn has shown that a negative linear compressibility, combined with a

---

R. H. Baughman and C. Cui, Allied Signal, Research and Technology, Morristown, NJ 07962–1021, USA.
S. Stafström, Department of Physics and Measurement Technology, Linköping University, S-581 83, Linköping, Sweden.
S. O. Dantas, Departamento de Fisica, UFJF, CEP 36036-330, Juiz de Fora, Minas Gerais, Brazil.

*To whom correspondence should be addressed. E-mail: ray.baughman@alliedsignal.com

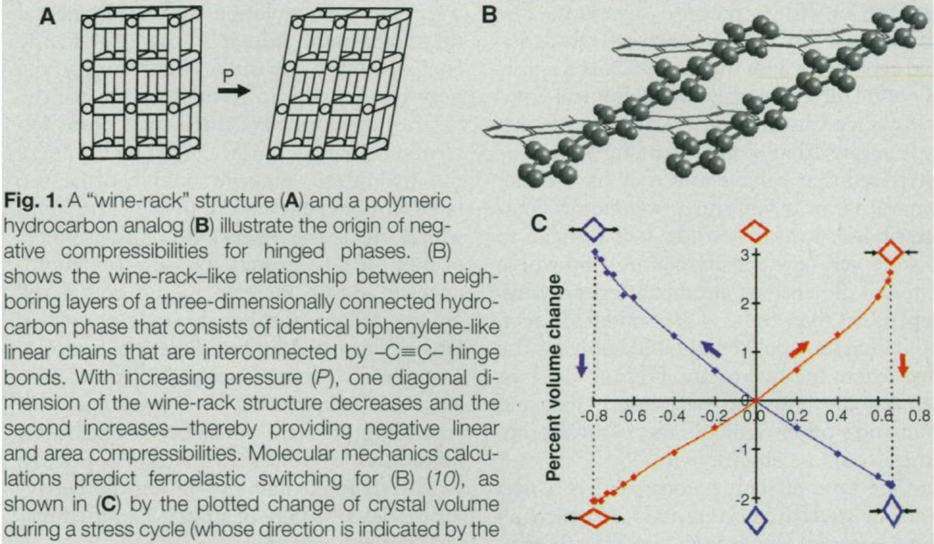

Fig. 1. A "wine-rack" structure (**A**) and a polymeric hydrocarbon analog (**B**) illustrate the origin of negative compressibilities for hinged phases. (B) shows the wine-rack–like relationship between neighboring layers of a three-dimensionally connected hydrocarbon phase that consists of identical biphenylene-like linear chains that are interconnected by –C≡C– hinge bonds. With increasing pressure (*P*), one diagonal dimension of the wine-rack structure decreases and the second increases—thereby providing negative linear and area compressibilities. Molecular mechanics calculations predict ferroelastic switching for (B) (*10*), as shown in (**C**) by the plotted change of crystal volume during a stress cycle (whose direction is indicated by the colored arrows). Rhombuses schematically indicate unit-cell shape before (red) and after (blue) a switching process that interchanges the two diagonal directions of the unit cell with respect to the stress direction (small arrows).

positive Grüneisen coefficient, can lead to a negative thermal expansion coefficient, but these properties need not coexist (*6*). Such negative linear thermal expansion coefficients are observed in the direction of maximum negative linear compressibility for Se, Te, β-phase *m*-dihydroxybenzene, cesium biphthalate, lanthanum niobate, and cesium dihydrogen phosphate, but the thermal expansion coefficients are all positive for Hg_2Br_2 and tris-sarcosine calcium chloride (*3, 6, 11, 12*).

Negative linear compressibilities result for various structures comprising helical chains: (i) single helices (Se and Te), (ii) oppositely wound helices like in the "finger cuff" child's toy (Fig. 2A), and (iii) the network of interconnected left- and right-handed helices observed (*11*) for β-phase *m*-dihydroxybenzene (Fig. 2B). Molecular mechanics calculations yield positive and negative linear compressibilities consistent with observations for β-phase *m*-dihydroxybenzene, and similar behavior for simpler compositions having the same network structure (*10*). The mechanical behavior of the finger cuffs (Fig. 2A) is like that of hinged-expansion wrist bands, and thus the finger cuffs can be viewed as a cylindrical type of hinged structure. Simple geometrical calculations show that a tensile stress in the helix axis direction decreases the volume of the finger cuff if the cylinder-direction angle between the helices is below 109.46°. Inversely, if the volume of a sealed finger cuff is filled with a fluid and the compressibility of the fluid differs from the linear compressibility of the helices, a negative linear compressibility can result for either the radial or axial direction (depending on the helix angle and the relative compressibilities of fluid and fiber). In fact, stretch densification has been shown for composites comprising a finger-cuff–like arrangement of high-modulus fibers in a much lower modulus polymer matrix (*13*). Because particular muscular hydrostats (such as found for nemertean, nematode, and turbellarian worms; squid tentacles; and ancient limbless tetrapods) have a similar structure (*14*), such biological structures may have negative linear compressibilities.

Plastically deformed foams and honeycombs are known (*15*) to provide either negative Poisson's ratios or Poisson's ratios whose sum exceeds unity about a stretch direction. The latter stretch-densified materials will have a negative linear compressibility for the special case where the hydrostatic compression fluid does not fill the pores.

The existence of solid materials with negative linear compressibilities (that is, stretch-densified materials) means that linear rods or fibers can be obtained whose length either (i) increases with increasing hydrostatic

Table 1. Characteristics of stretch-densified crystal phases are calculated from reported elastic compliance matrices (*7*). The minimum and maximum linear compressibilities, normalized with respect to the bulk compressibility (β_V), are $\beta_L(\min)/\beta_V$ and $\beta_L(\max)/\beta_V$. The axial directions of $\beta_L(\min)$ and $\beta_L(\max)$ are indicated in parentheses when these directions are symmetry axes. The column of Poisson's ratios is for the stretch axis providing maximum stretch densification, which coincides with the axis of minimum linear compressibility.

Crystal phase	$\beta_L(\min)/\beta_V$	$\beta_L(\max)/\beta_V$	Poisson's ratios (ν_{ij})	Comments on negative Poisson's ratios
		Trigonal		
Selenium	−0.25 (*c*)	0.62 (*a*)	$\nu_{31} = \nu_{32} = 0.93$	$\nu < 0$ and $\beta_L < 0$ for same stretch axis
Tellurium	−0.08 (*c*)	0.54 (*a*)	$\nu_{31} = \nu_{32} = 0.58$	$\nu < 0$ exists
		Tetragonal		
Mercurous iodide, Hg_2I_2	−0.13 (*c*)	0.56 (*a*)	$\nu_{31} = \nu_{32} = 0.89$	$\nu < 0$ and $\beta_L < 0$ for same stretch axis
Mercurous bromide, Hg_2Br_2	−0.05 (*c*)	0.52 (*a*)	$\nu_{31} = \nu_{32} = 0.61$	$\nu < 0$ and $\beta_L < 0$ for same stretch axis
		Orthorhombic		
3-Methyl 4-nitropyridine 1-oxide, $C_6N_2O_3H_6$	−0.44 (*b*)	0.83 (*c*)	$\nu_{21} = 0.56$, $\nu_{23} = 0.99$	$\nu < 0$ for crystal axes ($\nu_{13} = -0.91$, $\nu_{31} = -0.46$)
Cadmium formate, $Cd(COOH)_2$	−0.26 (*a*)	1.06 (*b*)	$\nu_{12} = 0.98$, $\nu_{13} = 0.28$	$\nu < 0$ exists
Calcium formate, $Ca(COOH)_2$	−0.21 (*a*)	0.74 (*b*)	$\nu_{12} = 0.80$, $\nu_{13} = 0.37$	$\nu < 0$ exists
m-Dihydroxybenzene, $C_6H_4(OH)_2$	−0.18 (*b*)	0.95 (*a*)	$\nu_{21} = 0.38$, $\nu_{23} = 0.83$	$\nu < 0$ exists
Cesium biphthalate, $C_6H_4COOHCOOCs$	−0.10 (*a*)	0.57 (*b*)	$\nu_{12} = 0.73$, $\nu_{13} = 0.38$	$\nu < 0$ exists
Tris-sarcosine calcium chloride, $(CH_3NHCH_2COOH)_3CaCl_2$	−0.07 (*b*)	0.69 (*a*)	$\nu_{21} = 0.76$, $\nu_{23} = 0.32$	$\nu < 0$ for crystal axes ($\nu_{13} = -0.07$, $\nu_{31} = -0.15$)
		Monoclinic		
Lanthanum niobate, $LaNbO_4$	−2.26	3.18	—	$\nu < 0$ and $\beta_L < 0$ for same stretch axis
Cesium dihydrogen phosphate, CsH_2PO_4	−1.36	2.23	—	$\nu < 0$ and $\beta_L < 0$ for same stretch axis
Ethylene diamine tartrate, $C_6H_{14}N_2O_6$	−0.10	0.85	—	$\nu < 0$ and $\beta_L < 0$ for same stretch axis

pressure or (ii) is pressure invariant. The latter possibility arises for any stretch-densified crystal, because there must exist a family of crystal directions in which the linear compressibility vanishes. The existence of such rods means that porous structures can be envisaged that behave as if they have either a negative or a vanishing volumetric compressibility. In other words, it is possible to make a very low-density porous solid whose external dimensions are much less pressure-dependent than those of diamond. However, this behavior would be obtained only for the case where the hydrostatic pressure fluid infiltrates the pores of the porous solid, and diamond's other desirable mechanical properties would be absent.

One type of such porous solid is a network of stretch-densified rods in which all three external dimensions are directly proportional to the length of an isolated rod. Because the volumetric compressibility of both the hydrostatic pressure fluid and the rods in the above porous networks are positive, there is no violation of the fundamental thermodynamic principle that volumetric compressibility is positive. Interestingly, the negative volumetric compressibility for the exterior dimensions of the above porous solid would change sign when the molecules of the hydrostatic pressure fluid become too large for pore penetration. In the latter limit, which yields the "jacketed compressibility" of Biot (*16*), hydrostatic pressure would produce an elastic increase in the crystal rod volume as long as the hydrostatic pressure is largely supported by rod-direction compressive stresses (along the stretch-densification axis). Such increasing crystal volume with increasing pressure would be observable by diffraction methods, and would appear to violate thermodynamics—unless the behavior we describe here of stretch-densified materials is recognized.

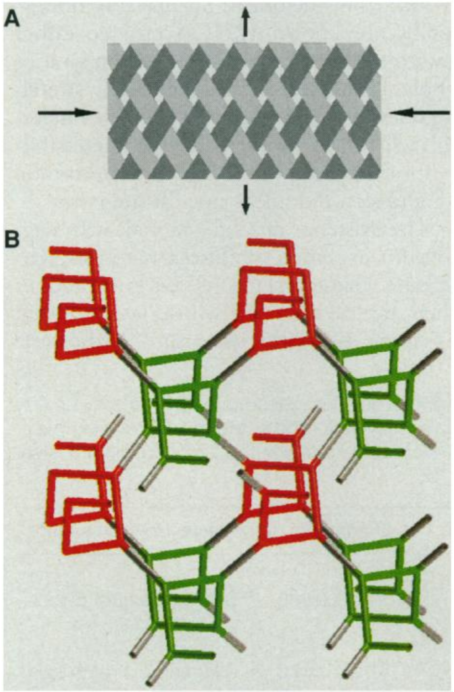

Fig. 2. Helical chain structures that provide stretch densification are illustrated. (**A**) shows the oppositely wound helices of a finger cuff, which has structural similarities to muscular hydrostats common for invertebrates (*14*). The arrows indicate the direction of pressure-induced dimensional changes for a muscular hydrostat (consisting of low-compressibility muscle fibers enclosing higher compressibility fluid-like components) when the helix-direction angle between the two helices is >109.46°. The network shown in (**B**) [consisting of interlinked chains of opposite chirality (red and green helices)] results for the stretch-densified phase of *m*-dihydroxybenzene when the OC_6H_4O linkage and the two hydrogen bonds to each end of this molecular linkage are each replaced by network bonds (*11*).

The above-described concept of using stretch-densified materials for the construction of effectively incompressible structures might find important applications for high-pressure environments. Examples are optical telecommunication line systems and sensor systems that must function miles deep in the ocean, where the pressure can exceed 1000 atm. Stretch-densified materials may also be used for increasing the sensitivity of pressure sensors (*17*). Consider interferometric optical sensors for sonar and aircraft altitude measurements, which use pressure-induced changes in optical path length. Device sensitivity is proportional to the fractional change in optical path length with pressure, which is a useful figure of merit. This equals the difference between the fractional change in refractive index with pressure and the linear compressibility. Because the refractive index normally increases with increasing density caused by a pressure increase, device sensitivity is decreased by term cancellation unless the linear compressibility is negative in the direction of light propagation. Furthermore, a linear compressibility can be giant in magnitude compared with the volume compressibility as a result of a negative linear compressibility. This means that very high figures of merit can be obtained by the use of optical materials having a negative linear compressibility. For example, the observed Pockels photoelastic constants, refractive indices, and elastic compliances of 3-methyl 4-nitropyridine 1-oxide (*18*) provide a maximum figure of merit (292 TPa^{-1}) that is 100 times higher than that for glass optical fiber. Also, materials having negative area compressibilities might be used as electrode clamps to provide order-of-magnitude sensitivity increases for ferroelectric pressure sensors. In this case, the pressure-induced expansion of the negative-area-compressibility material forces a ferroelectric sheet to increase area when pressure is applied, thereby eliminating the cancellation in the hydrostatic piezoelectric coefficient ($d_h = d_{33} + d_{31} + d_{32}$) caused by the opposite signs of d_{31} and d_{32} compared with d_{33}.

Because materials with negative linear compressibilities are so rare, we hope that these materials concepts will be used to extend this family and further optimize the achievable performance of important types of sensors. We also hope that this work will encourage the investigation of helix-based muscular hydrostats as negative compressibility systems and the generation of fluid-infiltrated porous structures with a lower effective compressibility than diamond.

REFERENCES AND NOTES

1. D. J. Gunton and G. A. Saunders, *J. Mater. Sci.* **7**, 1061 (1972).
2. B. Morosin and J. E. Schirber, *Solid State Commun.* **10**, 249 (1972).
3. J. W. E. Mariathasan, L. W. Finger, R. M. Hazen, *Acta Crystallogr. B* **41**, 179 (1985).
4. S. Prawer, T. F. Smith, T. R. Finlayson, *Aust. J. Phys.* **38**, 63 (1985).
5. E. F. Skelton, J. L. Feldman, C. Y. Liu, I. L. Spain, *Phys. Rev. B* **13**, 2605 (1976).
6. R. W. Munn, *J. Phys. C* **5**, 535 (1972).
7. *Low Frequency Properties of Dielectric Crystals*, vol. 29a of *Landolt-Börnstein, New Series, Group III*, D. F. Nelson, Ed. (Springer-Verlag, Berlin, 1993), and references therein for indicated compositions.
8. J. F. Nye, *Physical Properties of Crystals* (Oxford Univ. Press, Oxford, 1964), chap. 7, pp. 131–149.
9. R. H. Baughman and D. S. Galvão, *Nature* **365**, 735 (1993).
10. The calculations of Fig. 1C used the previously described molecular mechanics method (*9*). The calculations for *m*-dihydroxybenzene used Goddard's DREIDING force field [S. L. Mayo, B. D. Olafson, W. A. Goddard III, *J. Phys. Chem.* **94**, 8897 (1990)]. Consistent calculated and experimentally derived compressibilities (*7*) for volume (134 and 122 GPa^{-1}), *a* axis (110 and 116 GPa^{-1}), *b* axis (−41 and −22 GPa^{-1}), and *c* axis (66 and 28 GPa^{-1}) were obtained for β-phase *m*-dihydroxybenzene.
11. G. E. Bacon and E. J. Lisher, *Acta Crystallogr. B* **36**, 1908 (1980); A. F. Wells, *ibid.* **32**, 2619 (1976).
12. C. Barta *et al.*, *Sov. Phys. Crystallogr.* **24**, 608 (1979); K. Deguchi, E. Okaue, S. Ushio, E. Nakamura, *J. Phys. Soc. Jpn.* **53**, 3074 (1984); G. Sorge, U. Straube, N. R. Ivanov, *Phys. Status Solidi A* **65**, 189 (1981), S. F. Chistov, *Izv. Akad. Nauk Neorg. Mater.* **9**, 1749 (1973).
13. C. T. Herakovich, *J. Compos. Mater.* **18**, 447 (1984); P. J. Hine, R. A. Duckett, I. M. Ward, *J. Mater. Sci. Lett.* **16**, 541 (1997).
14. J. C. O'Reilly, D. A. Ritter, D. R. Carrier, *Nature* **386**, 269 (1997); W. M. Kier and K. K. Smith, *Zool. J. Linn. Soc.* **83**, 307 (1985).
15. L. J. Gibson, M. F. Ashby, G. S. Schajer, C. I. Robertson, *Proc. R. Soc. London. Ser. A* **382**, 25 (1982); R. Lakes, *Science* **235**, 1038 (1987); T. Lee and R. S. Lakes, *J. Mater. Sci.* **32**, 2397 (1997); A. Alderson and K. E. Evans, *ibid.* **30**, 3319 (1995); G. W. Milton, *J. Mech. Phys. Solids* **40**, 1105 (1992).
16. M. A. Biot, *J. Appl. Phys.* **33**, 1482 (1962); P. A. Berge and J. G. Berryman, *J. Appl. Mech.* **62**, 1053 (1995).
17. R. H. Baughman, Z. Iqbal, R. C. Morris, C. Cui, *Improved Sensors Based on Stretch-Densified Materials*, U.S. patent application pending.
18. J. Sapriel, R. Hierle, J. Zyss, H. Boissier, *Appl. Phys. Lett.* **55**, 2594 (1989).
19. We thank A. A. Zakhidov for useful discussions. S.O.D. thanks the Brazilian agency CAPES for financial support as visiting scholar.

10 November 1997; accepted 21 January 1998